Assessing *in Silico* Models and Methods for Non-Covalent Interactions between Graphene and Small Molecules

Christopher Ehlert*, Anna Piras, and Ganna Gryn'ova*

Heidelberg Institute for Theoretical Studies (HITS gGmbH), Schloss-Wolfsbrunnenweg 35, 69118 Heidelberg, Germany

Interdisciplinary Center for Scientific Computing (IWR), Heidelberg University, Im Neuenheimer Feld 368, 69120 Heidelberg, Germany

ABSTRACT

Designing and optimising graphene-based gas sensors, which involve physisorption of analytes on the sensor surface, requires theoretical insights into the strength and nature of such non-covalent interactions. This modelling entails constructing appropriate atomistic representations for an infinite graphene sheet and its complex with the analyte, then selecting accurate yet affordable methods for geometry optimisations and energy computations. In this work, density functionals from the 2nd to 5th rungs of Jacob's ladder, coupled cluster theory, and symmetry-adapted perturbation theory in conjunction with a range of surface models, from benzene to the periodic system, were tested for their ability to reproduce experimental adsorption energies of CO_2 on graphene in a low-coverage regime. The best agreement with the reference computations was found for global and double hybrid density functionals, while experimental adsorption energies were reproduced within chemical accuracy by extrapolating the SAPT0//DSD-BLYP-D3 interaction energies from finite clusters to infinity. This simple yet powerful extrapolation scheme effectively removes size dependence from the data obtained using finite cluster models, and the latter can be treated at more sophisticated levels of theory relative to periodic systems.

INTRODUCTION

Among practical applications of graphene – a two-dimensional sheet of sp[2]-carbon atoms arranged in a honeycomb lattice[1-3] – detection of small gaseous molecules is arguably the most readily geared towards viable real-life implementation.[4-8] Development and optimisation of graphene-based gas sensors, which typically operate *via* (non-)covalent interactions of adsorbates with the graphene surface, greatly benefit from theoretical insights into the strengths and nature of these interactions.[9] Examples of the properties studied *in silico* include adsorption geometries, energies, and charge transfer of small molecules (H_2O, NO, NO_2, NH_3, and CO) adsorbed on graphene,[10] selectivity of NH_3 detection with graphene nanoribbons,[11] and the role of surface defects in the adsorption of CO_2 and CO on graphene.[12] In these studies, graphene and its derivatives were modelled as periodic systems, however, an infinite graphene sheet can instead be represented by a finite molecular fragment. For example, in a joint theoretical and experimental study on the adsorption of organic molecules on graphene, averaged *ab initio* molecular dynamics energies obtained with non-local van der Waals functionals were in excellent agreement with empirical data.[13]

Choosing an appropriate model of the adsorbate-surface complex in conjunction with an electronic structure theory method, which affords an efficient sampling of adsorption geometries for a given adsorbate concentration regime, is a key to accurately simulate graphene-based gas sensors.[9] Periodic representation of the surface can be advantageously free of defects and edge effects; yet, on an *ab initio* level it is usually feasible only at the local density or generalised gradient approximations (LDA and GGA, respectively) of density functional theory (DFT), which cannot describe dispersive interactions without empirical corrections or non-local functional extensions. While more high-level density functionals, periodic second-order perturbation theory (MP2), random phase approximation (RPA), and the GW approach are available and able to address the aforementioned limitations of LDA and

GGA DFT, they generally come at a prohibitively high computational cost.[9] This is particularly the case for adsorption in the low coverage regime, where large surface slab models are required in addition to large vacuum gaps along the normal directions of the surfaces. Finite cluster models, on the other hand, can be treated with a broad spectrum of wavefunction-based methods, as well as density functionals from the higher rungs of Jacob's ladder.[14] Unfortunately, these models suffer from artificial edge effects and heavy size-dependence of their computed properties.

In the absence of a realistic yet computationally inexpensive model, what is the most balanced approach to simulating the adsorption of gas molecules on graphene? To address this question, we assessed the performance of diverse electronic structure theory methods across the surface model sizes for adsorption geometries and energies of CO_2 on graphene. *In silico* findings were corroborated *via* comparison with the results from two recent experimental studies. In a study by Matsuda *et al.*,[15] adsorption of carbon dioxide on a monolayer of epitaxial graphene on a SiC(0001) surface was analysed by temperature-programmed desorption (TPD) and X-ray photoelectron spectroscopy (XPS). At low CO_2 coverage, the adsorption energy was found to be 30.1 ± 1.5 kJ mol^{-1}, decreasing to 25.4 ± 1.5 kJ mol^{-1} at higher coverages. The XPS results indicated blue shifts of the O 1s and C 1s electron binding energies with increasing adsorbate coverage. Additional periodic density functional theory computations using non-local van der Waals exchange correlation functionals suggested that CO_2 is adsorbed parallel to the surface. In a more recent study by Smith and Kay,[16] a binding energy of 26.1 ± 2 kJ mol^{-1} was reported for low CO_2 coverage on graphene exposed on a Pt(111) surface. While this value is close to that reported by the first study,[15] the results of reflection adsorption infrared spectroscopy (RAIRS) suggested that CO_2 is instead tilted away from the surface. Furthermore, the vibrational band of the antisymmetric stretch mode of CO_2, which is located at 2350 cm^{-1} at low coverage, is blue-shifted to 2378 cm^{-1} upon transition to higher coverages.

In this study, we test the ability of various simulation approaches to reproduce the reported experimentally measured adsorption energies and analyse the adsorption geometries of carbon dioxide on graphene in a low coverage regime. Examined methodological approaches span from the smallest possible graphene model, benzene, treated at various approximations to the DFT exchange-correlation functional and at highly accurate wavefunction-based methods, to the realistic periodic representation of graphene in conjunction with a GGA density functional.

COMPUTATIONAL DETAILS

Chemical model. The structures of the finite models of graphene investigated here (Figure 1A) can be categorised based on their edge structures and shapes as circular (benzene, coronene, and circumcoronene), zigzag (rhomboid shapes), and armchair (rectangular shapes). For each of these models, three principal adsorption sites (top, hollow, and bridge, shown in Figure 1B for benzene) are considered in parallel (shown in Figure 1B) and orthogonal orientations. In the larger systems, CO_2 is located either near the central C–C bond (for 2×2-zigzag, 4×4-zigzag, 3×2-armchair), or near the central 6-membered ring. Constrained optimisations were performed to preserve the initial adsorption geometries, since they do not necessarily correspond to the local minima on the potential energy surface (PES); the corresponding structures and their energies were then compared to those in the fully relaxed minima, obtained in unconstrained optimisations and confirmed by normal mode analyses.
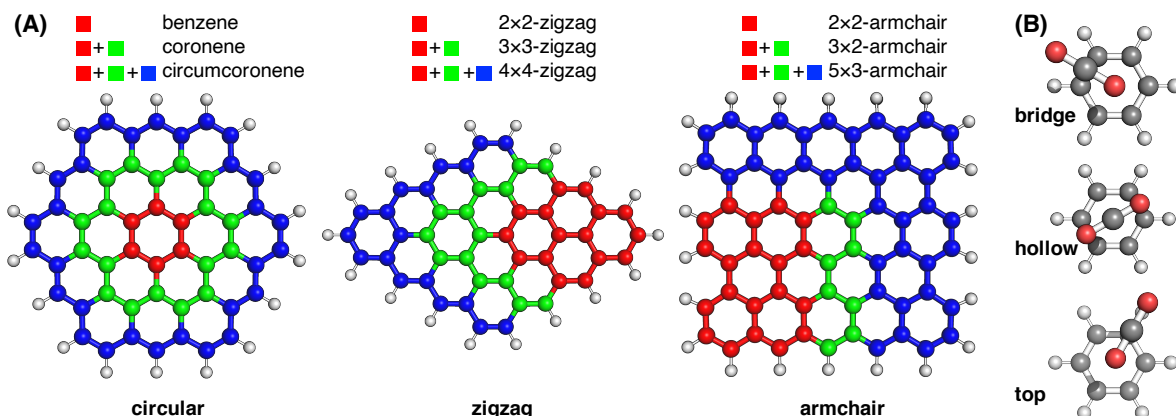
Figure 1. (A) Graphene surface models: the smallest model in red, a mid-sized model in red and green, and a large model in red, green, and blue. (B) Principal adsorption sites are shown for a parallel orientation of CO_2 on benzene.

Finite model. The following DFT methods in combination with appropriate dispersion corrections were used in geometry and energy computations: generalised density approximation functional PBE-D3,[17,18] hybrid-GGA functional B3LYP-D3,[19,20] the long-range separated functional ωB97X-D3[21] and its non-local version ωB97X-V[22] for single-point energies, and the double hybrid functional DSD-BLYP-D3.[23] The latter two functionals were found to be among the best for describing inter- and intramolecular non-covalent interactions.[24] All DFT computations were performed with a recent version of the ORCA program[25] using *very tight* convergence thresholds and the largest DFT grids (keyword: GRID7). See the Supporting Information (SI) for a sample input. Coupled cluster with singles, doubles, and perturbative triples (CCSD(T)) computations were performed using the XNCC module of the CFOUR program.[26,27] ORCA's capability to function as an external optimiser was utilised to perform geometry optimisations with Cartesian coordinates with and without constraints using the exact same convergence criteria as for the DFT computations. A self-written interface using Atomic Simulation Environment (ASE)[28] was used to transform the gradients between the input orientation and CFOUR's standard orientation. The symmetry-adapted perturbation

6

theory (SAPT)[29-31] computations at a SAPT0 level in conjunction with DFT geometries were performed using Psi4.[32,33] The SAPT0 results are relatively independent on the DFT functional used to obtain the geometries (see Table S4 in the SI), thus data based on the PBE-D3 geometries are reported herein. Unless stated otherwise, all computations were performed with the def2-TZVP basis set.[34,35]

The interaction energy is computed as the difference between the energies of the optimised dimer and the two monomers in their dimer geometries:

$$E_{int} = E^D_{graphene/CO_2}(D) - E^D_{CO_2}(D) - E^D_{graphene}(D) \qquad \text{Eq. 1,}$$

where $E^D_X(D)$ is the energy of the fragment X in the dimer geometry using the dimer basis set. Computations for the monomer fragments are performed using the basis set of the dimer so as to correct for the basis set superposition error (BSSE). Importantly, computed interaction energies are always slightly lower than the experimental adsorption energies, since the latter contain additional, albeit relatively small in non-covalently bound complexes, relaxation effects (or deformation energy) of the monomers.

Periodic model. Computations on an infinite/periodic model of graphene were performed at the PBE-D3 level using the QuantumEspresso program.[36] A 7×7 supercell approach with 98 carbon atoms and pseudopotentials from the PSLibrary[37] was used. An energy cutoff of 90 Ry for the plane-wave expansion of the wavefunction was selected after careful evaluation of the interaction energy dependence on the cutoff value (see Figure S1 in the SI). For this cell size, no dependence on the number of included k-points was detected (see Table S2 in the SI); therefore, all computations were executed at the Γ-point. In contrast to the finite cluster systems, no constraints were needed, since initial adsorption geometries were preserved throughout optimisations. The systems were optimised until the maximum force exerted on an atom was below 0.01 eV Å^{-1}, using the ASE interface with QuantumEspresso.

RESULTS AND DISCUSSION

Method assessment: Energies. Interaction energies for CO_2 adsorbed on benzene, computed according to Eq. 1 using a range of DFT and wavefunction theory methods for global minima and diverse constrained orientations, are shown in Table 1. Among all tested electronic structure methods, CCSD(T) results in the lowest absolute interaction energies, while SAPT0 gives the most stable complexes, especially for parallel adsorption. The likely origins of this discrepancy are (*i*) the basis set effects on the CCSD(T) energies, and (*ii*) the low order of the perturbation expansion used for SAPT. To confirm this, we performed DLPNO-CCSD(T)[38] and higher order SAPT single point computations for a fixed geometry and with larger basis sets (see Table S5 in the SI). The biggest difference between the two methods using a larger basis (def2-QZVPPD) and a higher order of perturbation (SAPT2+3) is only 2.3 kJ mol^{-1}. Considering the DFT results, all computed E_{int} are relatively close to each other and to the reference coupled cluster and SAPT0 computations. The relative order of interaction energies across adsorption geometries is the same for all DFT methods. For example, among the parallel orientations, the bridge sites have the lowest E_{int}, followed by the top and hollow geometries. This trend is also in agreement with the SAPT0 results; however, the hollow adsorption site is more stable than the top adsorption site at the CCSD(T) level, albeit only by 0.2 kJ mol^{-1}. For the orthogonal geometries, the hollow adsorption site is predicted to be the most stable at all considered DFT and wavefunction theory methods. Among the DFT functionals, the double-hybrid DSD-BLYP-D3 gives results that are closest to the coupled cluster, while the long-range separated hybrid ωB97X-D3 most closely reproduces the SAPT0 computations. These observations are in agreement with the broader trends from an extensive benchmarking study by Grimme *et al.*,[24] exemplified by, e.g., the mean deviations for the S66 test set (in kJ mol^{-1}): 1.13 (PBE-D3), 1.05 (B3LYP-D3), 0.96 (ωB97X-D3), 0.17 (ωB97X-V) and 0.04 (DSD-BLYP-D3). Nonetheless, all computed E_{int} values are significantly lower than the reported

experimental adsorption energies for CO_2 on graphene (30.1 ± 1.5 kJ mol^{-1} and 26.1 ± 2 kJ mol^{-1}),[15,16] suggesting that larger models might be needed to reproduce these values.
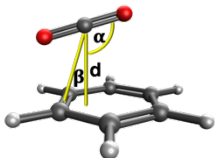
Table 1. Computed interaction energies (in kJ mol^{-1}) for CO_2 on benzene at various adsorption sites and orientations.

Method/def2-TZVP	Global minima	Local minima (constrained optimisation)					
		Parallel orientation			Orthogonal orientation		
		bridge	top	hollow	bridge	top	hollow
CCSD(T)	-7.6	-7.2	-6.9	-7.1	-0.4	-0.4	-0.5
SAPT0//PBE-D3	-11.9	-11.4	-10.9	-10.7	-1.0	-1.1	-1.4
PBE-D3	-10.2	-9.9	-9.6	-9.5	-1.7	-1.7	-2.1
B3LYP-D3	-10.9	-10.5	-10.2	-10.0	-0.9	-0.9	-1.3
ωB97X-D3	-11.3	-10.9	-10.5	-10.3	-1.0	-1.0	-1.5
ωB97X-V	-10.6	-10.2	-9.8	-9.8	-1.2	-1.2	-1.8
DSD-BLYP-D3	-9.2	-8.8	-8.4	-8.4	-0.8	-0.8	-1.1

Method assessment: Geometries. Considering the specific adsorption geometries, parallel orientations are significantly more stable than the orthogonal ones independent of the computational method. For a given parallel orientation, top and bridge sites are very close in energy, while the hollow site is on average approximately 0.5 kJ mol^{-1} less stable. To further analyse the adsorption geometries, the following parameters have been analysed: distance d between the adsorption site (benzene ring plane) and the CO_2 molecule (carbon or oxygen atom in case of parallel or orthogonal adsorption, respectively), tilt angle α between the CO_2 axis and the surface plane, and angle β representing an angle between the adsorption site, CO_2 centre of mass (*i.e.*, the carbon atom) and its projection onto the surface plane (Table 2). Within the constrained geometries, the bridge and top sites in the parallel orientation feature very similar distances d, which are consistently larger by approximately 0.17 Å in hollow geometries. The

converse is evident for orthogonal orientations, where the hollow adsorption occurs at a shorter range relative to the top and bridge counterparts. These structural trends reflect the corresponding interaction energies (Table 1): the top and bridge adsorptions are more stable for parallel, but less stable for the orthogonal orientations compared to the hollow adsorptions. The global minimum geometries are generally very similar to the bridge parallel adsorption site; however, the CO_2 in the former is slightly shifted towards the centre of the ring, as indicated by the β angle.

Table 2. Geometrical parameters across adsorption sites of CO_2 on benzene, computed with different electronic structure methods. The inset figure illustrates these parameters.

	Global minima			Local minima (constrained optimisation)					
				Parallel orientation			Orthogonal orientation		
				bridge	top	hollow	bridge	top	hollow
Method/def2-TZVP	α,°	β,°	d, Å	d, Å					
CCSD(T)	92.5	3.8	3.25	3.24	3.24	3.40	3.41	3.42	3.27
PBE-D3	93.8	1.6	3.30	3.30	3.29	3.47	3.46	3.46	3.36
B3LYP-D3	93.3	2.1	3.25	3.25	3.24	3.40	3.44	3.43	3.29
ωB97X-D3	93.2	2.2	3.21	3.22	3.21	3.38	3.45	3.46	3.33
DSD-BLYP-D3	92.5	3.2	3.24	3.23	3.23	3.39	3.40	3.40	3.26

Among the tested DFT methods, PBE consistently predicts the greatest adsorption distances, while the shortest d is obtained with ωB97X-D3 for parallel, and with DSD-BLYP-D3 for orthogonal orientations. Compared to the CCSD(T) reference, all density functionals predict qualitatively correct trends. However, PBE-D3 results tend to overestimate d by 0.5-0.9 Å for all adsorption geometries, likely due to its neglect of the Hartree-Fock-like exact exchange.[39] Geometries obtained with the global hybrid B3LYP-D3 and the long-range separated ωB97X-

D3 are closer to the CCSD(T) geometries than those computed using PBE-D3. Finally, the double hybrid functional DSD-BLYP-D3 reproduces the CCSD(T) geometries most accurately, with a maximum deviation of only 0.02 Å.

Overall, the double hybrid functional DSD-BLYP-D3 predicts geometries and energies that are the closest to the CCSD(T) reference, in line with the recent benchmark study.[24] However, the scaling of its computational cost is less favourable compared to B3LYP-D3 and ωB97X-D3.[39,40] This factor, whilst insignificant for a relatively compact benzene•••CO_2 complex, can become crucial when moving towards larger and more realistic surface models.

Size dependency. How transferrable is the computed interaction energy of carbon dioxide with benzene to the infinite graphene sheet? To address this, we have tested the size dependency of E_{int} computed with different DFT methods across a range of cluster models (Figure 1) up to periodic graphene; for clarity, only the PBE-D3 results are detailed further (Table 3, the corresponding geometrical parameters and the results of other methods can be found in Tables S1 and S4 of the SI).

Table 3. Size dependency of the interaction energies (in kJ mol^{-1}) of CO_2 on multiple graphene models computed with PBE-D3.

Model	No. of carbon atoms	Global minima	Local minima (constrained optimisation)					
			Parallel orientation			Orthogonal orientation		
			bridge	top	hollow	bridge	top	hollow
Benzene	6	-10.2	-9.9	-9.6	-9.5	-1.7	-1.7	-2.1
Coronene	24	-13.9	-13.9	-13.2	-12.8	-6.0	-5.8	-6.9
Circumcoronene	54	-15.4	-15.4	-14.6	-14.0	-7.6	-7.5	-8.2
2×2-zigzag	16	-13.1	-13.1	-12.3	-11.4	-5.1	-4.9	-4.9
3×3-zigzag	30	-14.3	-14.2	-13.6	-13.1	-6.3	-6.4	n/a ^{a}
4×4-zigzag	48	-15.2	-15.2	-14.5	-13.8	-7.4	-7.4	-7.8

2×2-armchair	20	-13.3	-13.3	-13.0	-12.2	-5.2	-5.2	-6.2
3×2-armchair	28	-14.4	-14.4	-13.7	-12.8	-6.6	-6.4	-6.9
5×3-armchair	66	-15.5	-15.5	-14.8	-14.0	-7.7	-7.6	-8.3
Extrapolated		-16.3	-16.3	-15.6	-14.9	-8.6	-8.6	-9.4
Periodic		-15.6	-15.6	-15.2	-14.4	-8.5	-8.5	-9.0

[a] (Constraint) minimum structure that preserved the initial characteristics was not located.

The following observations can be made on the basis of these results:

1. *Larger surface models lead to more stable clusters* independent of the computational method and the adsorption geometry. On average, the interaction energies are lower by 6-8 kJ mol^{-1} for the largest considered graphene models compared to the smallest ones. Furthermore, this increase in the stability of CO_2•••graphene complexes is accompanied by shorter interaction distances (see Table S1 in the SI), albeit to an extent dependent on the adsorption site. For instance, these distances decrease by only 0.06 Å (from 3.30 Å for benzene to 3.24 Å for the 5×3-armchair model) in the bridge parallel adsorptions, but by 0.26 Å (from 3.36 Å for benzene to 3.10 Å for the 5×3-armchair model) for the hollow orthogonal counterparts. In general, the orthogonal adsorption geometries are more strongly affected by the increasing model size than their parallel equivalents. A similar correlation between larger graphene models and shorter adsorption distances was reported by Irle *et al.*[41]

2. *The relative order of interaction energies does not depend on the system size.* For example, the bridge parallel adsorption is always the most stable complex (optimised under constraint), followed by the top and hollow parallel orientations. Similarly, the hollow adsorption site is the most stable among orthogonal orientations (except for the 2×2-zigzag model).

3. *All larger models (circumcoronene, 3×3-zigzag, and 5×3-armchair) converge to similar adsorption geometries.* For example, all large models feature similar CO_2•••surface distances for the bridge parallel adsorption (see Table S1 in the SI).

4. *Geometries of all global minima are similar to each other* and very similar to the bridge parallel adsorption.

5. *The interaction energy is approximately linearly proportional to the inverse size of the surface model (beyond benzene)*, *i.e.,* the inverse of the number of carbon atoms it contains (PBE-D3 data is shown in Figure 2, while the plots for other functionals are given in Figure S2 of the SI). The linear fit of this data intercepts the *y*-axis at $\lim_{x \to \infty} m/x + n$, where x is the number of carbon atoms in the surface model. Similar extrapolation schemes have been established for E_{int} of graphene with water (exponential fit),[42] acetone (three-parameter exponential fit),[41] a second graphene layer,[43] and nucleobases[44] (non-linear two parameter fits). Importantly, such an extrapolation scheme gives interaction energies for an artificial, infinitely large graphene model at any quantum-chemical method applicable to finite systems (Table 4). Extrapolated PBE-D3 E_{int} values are within 1 kJ mol^{-1} from the periodic PBE-D3 results, strongly suggesting that this extrapolation scheme is verily capable of capturing the energetics of non-covalent interactions for an infinitely large surface model.
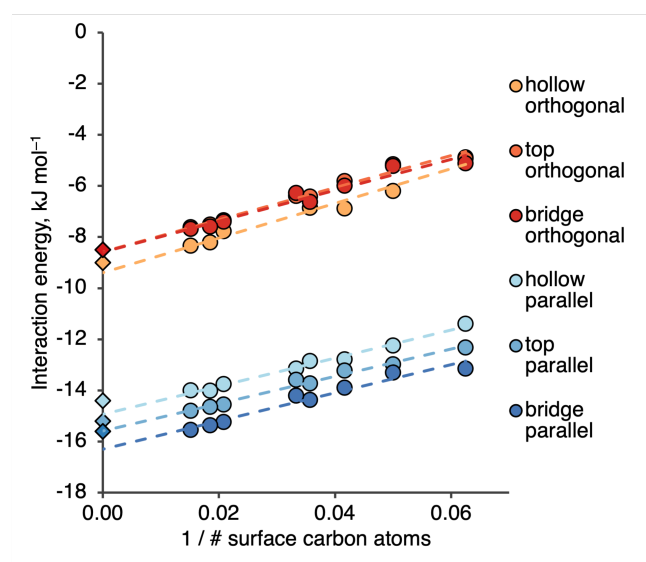

Figure 2. PBE-D3 interaction energies of CO_2 as a function negatively correlated with the number of carbon atoms in the underlying finite surface model (circles), corresponding PBE-

D3 E_{int} for the periodic model (diamonds), and linear regression fits of the finite model data points (dashed lines).

Extrapolated values for the interaction of carbon dioxide with an artificial infinite graphene sheet follow the same trends in terms of preferred adsorption geometries at all methods considered (Table 4). The bridge parallel adsorption site is the most stable and converges to the values obtained for the global minimum adsorptions. The highest E_{int} values are obtained with periodic and cluster-based PBE-D3 computations, and while they are close to each other, they are approximately 10 kJ mol^{-1} greater than the experimental adsorption energies. Among the DFT methods, B3LYP-D3 gives the lowest extrapolated interaction energy (-19.8 kJ mol^{-1} for the global minimum), in reasonable agreement with the empirical data (30.1 ± 1.5 kJ mol^{-1} and 26.1 ± 2 kJ mol^{-1}).[15,16]

Table 4. Extrapolated interaction energies (in kJ mol^{-1}) of CO_2 adsorbed on an artificial infinite graphene model computed with several density functionals and SAPT0.

| Method | Global minima | Local minima (constrained optimisation) | | | | | |
| | | Parallel orientation | | | Orthogonal orientation | | |
		bridge	top	hollow	bridge	top	hollow
PBE-D3	-16.3	-16.3	-15.6	-14.9	-8.6	-8.6	-9.4
B3LYP-D3	-19.8	-19.8	-18.8	-18.0	-9.5	-9.5	-10.6
ωB97X-D3	-17.9	-17.8	-16.6	-15.8	-8.4	-8.4	-9.5
ωB97X-V	-18.6	-18.6	-17.4	-16.7	-9.7	-9.7	-10.4
DSD-BLYP-D3	-18.9	-18.9	-18.0	-17.3	-10.8	-10.3	-11.6
SAPT0//PBE-D3	-24.8	-24.8	-23.2	-22.0	-14.2	-14.1	-15.9
SAPT0//B3LYP-D3	-25.7	-25.6	-23.9	-22.7	-14.7	-14.5	-16.5
SAPT0//ωB97X-D3	-25.6	-25.5	-23.8	-22.6	-14.3	-14.2	-16.1
SAPT0//DSD-BLYP-D3	-27.0	-26.8	-25.1	-23.8	-16.2	-15.2	-18.2

PBE-D3 (periodic)	-15.6	-15.2	-14.4	-8.5	-8.5	-9.0

The interaction energies obtained with SAPT0 are even lower than the B3LYP-D3 values and are closer to experimental adsorption energies. The extrapolated E_{int} for the global minimum at the DSD-BLYP-D3 geometry is -27.0 kJ mol^{-1}, in excellent agreement with the experimental observations.[15,16] With respect to the underlying geometries, SAPT0 interaction energies are the highest for the PBE-D3 geometries, and lowest for the DSD-BLYP-D3 structures. However, the difference between these results is rather small (< 2 kJ mol^{-1}) and is a direct outcome of the corresponding adsorption distances (see discussion and Table S3 in the SI).

Established extrapolation using a combination of density functional theory and symmetry-adapted perturbation theory represents a simple yet powerful scheme for obtaining accurate interaction energies for CO_2 with graphene. Such a linear fit across model sizes has been demonstrated to be necessary to arrive at the most stable complexes and the interaction energies that are the closest to experimental values. The best agreement is obtained for geometries optimised with the DSD-BLYP-D3 method and energies evaluated at SAPT0 level. However, results nearly as accurate can be obtained with computationally less expensive functionals used for geometry optimisations.

Nature of the interactions. Symmetry-adapted perturbation theory provides not only highly accurate total non-covalent interaction energies, but also the ability to decompose them into physically meaningful components.[31] As might be expected for interactions between neutral organic molecules,[45] dispersion is a primary stabilising force in the investigated complexes, supplemented by attractive electrostatics and countered by repulsive exchange (Figure 3A). This qualitative behaviour is observed in all studied adsorption geometries (see further discussion and Figures S3-4 in the SI). Considering the size dependence of the energy

contributions, beyond benzene induction and electrostatic terms are constant and independent of the system size, while exchange and dispersion become larger (on an absolute scale) with increasing system size. When carbon dioxide transitions from a parallel to an orthogonal orientation, the absolute values of all E_{int} components decrease (Figure 3B). This change is most profound for the attractive contributions, leading to an overall weaker interaction for the orthogonally oriented CO_2 on graphene.
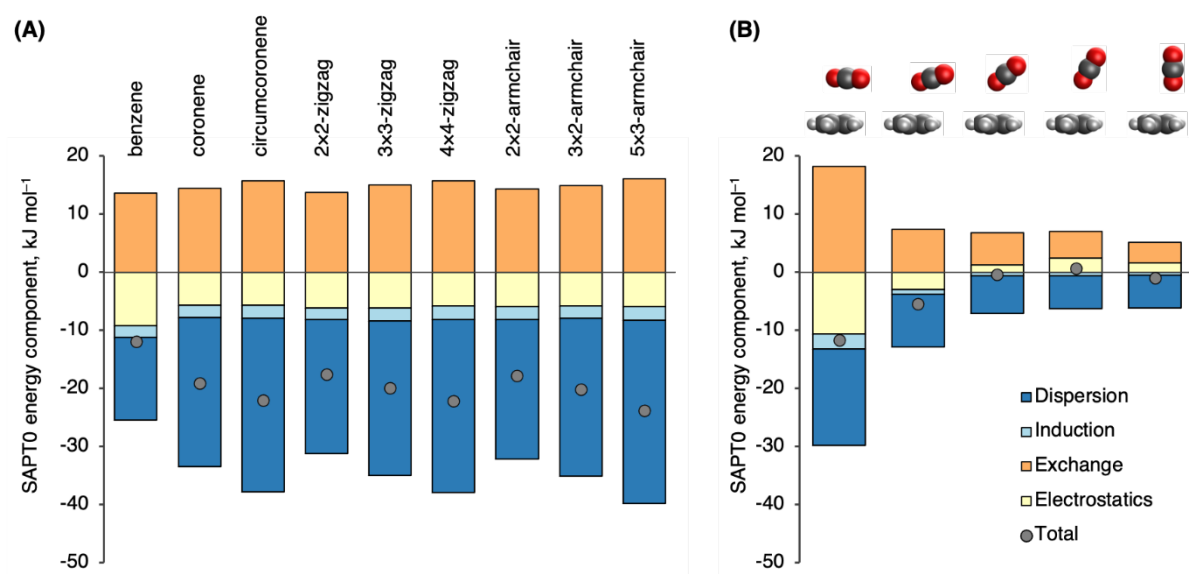
Figure 3. Energy decomposition analysis of the SAPT0//PBE-D3 total interaction energies in CO_2 complexes (A) with various surface models (global minima adsorption geometries), as well as (B) along the transition between the parallel and orthogonal bridge adsorption of CO_2 on benzene (the intermediate points were found by a linear interpolation of the coordinates between the two PBE-D3 stationary points).

CONCLUSION AND OUTLOOK

In search of an optimal methodological approach to modelling the absorption of small gaseous molecules on two-dimensional organic materials, the ability of various density functional theory and wavefunction theory methods, as well as finite and periodic models to

reproduce experimental adsorption energies of carbon dioxide on graphene has been probed. For the smallest model, benzene, a comparison with the gold standard of quantum chemistry, CCSD(T), shows that the double-hybrid DSD-BLYP-D3 functional performs the best, in accordance with previous benchmarks. Nonetheless, all computed interaction energies for $CO_2\cdots$benzene complexes are relatively far from the experimental adsorption energies of CO_2 on graphene in a low coverage regime. Even with larger cluster models (up to 66 carbon atoms), computed DFT interaction energies are underestimated by 10-20 kJ mol^{-1} with respect to experiment. Instead, a simple linear fit extrapolating the interaction energies of CO_2 on a model surface from finite clusters to infinity and using a combination of density functional theory and symmetry-adapted perturbation theory produces interaction energies in excellent agreement with the experimental values. Computed energies of these dispersion-driven interactions are consistently lower (*i.e.,* more stable) in complexes with shorter distances between CO_2 and the surface model. Relative stabilities of the considered adsorption geometries are generally independent of the density functional and the cluster size, with parallel orientations being generally more stable than their orthogonal counterparts. Interaction energies obtained in conjunction with the PBE-D3 geometries are the furthest from the reference values, followed by B3LYP-D3 and ωB97X-D3. DSD-BLYP-D3 predicts the shortest adsorption distances, which, combined with SAPT0 interaction energies, predict the most stable complexes. Thus, while reasonable relative adsorption energies can be obtained at a relatively low computational cost with medium-sized graphene clusters using PBE-D3, reliable estimates of absolute adsorption energies require a combination of higher-level DFT (e.g., DSD-BLYP-D3) geometries with SAPT0 energies, extrapolated to the infinite cluster size limit. Beyond graphene-based sensors for carbon dioxide, these findings can be used as a general recipe for computational modelling of various small molecules on graphene and other two-dimensional organic materials.

ASSOCIATED CONTENT

Supporting Information. The Supporting Information is available free of charge:

Sample ORCA input, evaluation of plane-wave cutoff and k-point in periodic computations, complete set of computed size-dependent geometrical and energetic data, figures and tables with additional computations at higher-order SAPT, DLPNO-CCSD(T), and larger basis sets, linear fits of size-dependent interaction energies for all tested methods, additional SAPT0 energy decomposition analyses (PDF).

Electronic energies of the studied complexes (XLXS).

Geometries of the studied complexes (XYZ).

AUTHOR INFORMATION

Corresponding Authors

*Christopher Ehlert – *Heidelberg Institute for Theoretical Studies (HITS gGmbH), Schloss-Wolfsbrunnenweg 35, 69118 Heidelberg, Germany, and Interdisciplinary Center for Scientific Computing (IWR), Heidelberg University, Im Neuenheimer Feld 368, 69120 Heidelberg, Germany*; orcid.org/0000-0002-6296-8733; E-mail: christopher.ehlert@h-its.org.

*Ganna Gryn'ova – *Heidelberg Institute for Theoretical Studies (HITS gGmbH), Schloss-Wolfsbrunnenweg 35, 69118 Heidelberg, Germany, and Interdisciplinary Center for Scientific Computing (IWR), Heidelberg University, Im Neuenheimer Feld 368, 69120 Heidelberg, Germany*; orcid.org/0000-0003-4229-939X; E-mail: ganna.grynova@h-its.org.

Author

Anna Piras – *Heidelberg Institute for Theoretical Studies (HITS gGmbH), Schloss-Wolfsbrunnenweg 35, 69118 Heidelberg, Germany, and Interdisciplinary Center for Scientific Computing (IWR), Heidelberg University, Im Neuenheimer Feld 368, 69120 Heidelberg, Germany*; orcid.org/0000-0002-1528-8874; E-mail: anna.piras@h-its.org.

Author Contributions

Christopher Ehlert: investigation, methodology, formal analysis, writing-initial draft, review, and editing; **Anna Piras**: investigation, formal analysis, writing-review, and editing; **Ganna Gryn'ova**: conceptualisation, supervision, formal analysis, writing-review, and editing.

Notes

The authors declare no competing financial interest.

REFERENCES

1 Novoselov, K. S.; Geim, A. K.; Morozov, S. V.; Jiang, D.; Zhang, Y.; Dubonos, S. V.; Grigorieva, I. V.; Firsov, A. A. Electric Field Effect in Atomically Thin Carbon Films. *Science* **2004**, *306*, 666-669. DOI: 10.1126/science.1102896.

2 Georgakilas, V.; Otyepka, M.; Bourlinos, A. B.; Chandra, V.; Kim, N.; Kemp, K. C.; Hobza, P.; Zboril, R.; Kim, K. S. Functionalization of Graphene: Covalent and Non-Covalent Approaches, Derivatives and Applications. *Chem. Rev.* **2012**, *112*, 6156-6214. DOI: 10.1021/cr3000412.

3 Yu, X.; Cheng, H.; Zhang, M.; Zhao, Y.; Qu, L.; Shi, G. Graphene-Based Smart Materials. *Nat. Rev. Mater.* **2017**, *2*, 17046. DOI: 10.1038/natrevmats.2017.46.

4 Shao, Y.; Wang, J.; Wu, H.; Liu, J.; Aksay, I. A.; Lin, Y. Graphene Based Electrochemical Sensors and Biosensors: A Review. *Electroanalysis* **2010**, *22*, 1027-1036. DOI: 10.1002/elan.200900571.

5 Schedin, F.; Geim, A. K.; Morozov, S. V.; Hill, E. W.; Blake, P.; Katsnelson, M. I.; Novoselov, K. S. Detection of Individual Gas Molecules Adsorbed on Graphene. *Nature Mater.* **2007**, *6*, 652-655. DOI: 10.1038/nmat1967.

6 Singh, E.; Meyyappan, M.; Nalwa, H. S. Flexible Graphene-Based Wearable Gas and Chemical Sensors. *ACS Appl. Mater. Interfaces* **2017**, *9*, 34544-34586. DOI: 10.1021/acsami.7b07063.

7 Choi, J. H.; Lee, J.; Byeon, M.; Hong, T. E.; Park, H.; Lee, C. Y. Graphene-Based Gas Sensors with High Sensitivity and Minimal Sensor-to-Sensor Variation. *ACS Appl. Nano Mater.* **2020**, *3*, 2257-2265. DOI: 10.1021/acsanm.9b02378.

8 Yuan, W.; Shi, G. Graphene-Based Gas Sensors. *J. Mater. Chem. A* **2013**, *1*, 10078-10091. DOI: 10.1039/C3TA11774J.

9 Piras, A.; Ehlert, C.; Gryn'ova, G. Sensing and Sensitivity: Computational Chemistry of Graphene-Based Sensors. *WIREs Comput. Mol. Sci.* **2021**, Early View. DOI: 10.1002/wcms.1526.

10 Leenaerts, O.; Partoens, B.; Peeters, F. M. Adsorption of H_2O, NH_3, CO, NO_2, and NO on Graphene: A First-Principles Study. *Phys. Rev. B* **2008**, *77*, 125416. DOI: 10.1103/PhysRevB.77.125416.

11 Huang, B.; Li, Z.; Liu, Z.; Zhou, G.; Hao, S.; Wu, J.; Gu, B.-L.; Duan, W. Adsorption of Gas Molecules on Graphene Nanoribbons and Its Implication for Nanoscale Molecule Sensor. *J. Phys. Chem. C* **2008**, *112*, 1344213446. DOI: 10.1021/jp8021024.

12 Tit, N.; Said, K.; Mahmoud, N. M.; Kouser, S.; Yamani, Z. H. Ab-Initio Investigation of Adsorption of CO and CO_2 Molecules on Graphene: Role of Intrinsic Defects on Gas Sensing. *Appl. Surf. Sci.* **2017**, *394*, 219-230. DOI: 10.1016/j.apsusc.2016.10.052.

13 Lazar, P.; Karlický, F.; Jurečka, P.; Kocman, M.; Otyepková, E.; Šafářová, K.; Otyepka, M. Adsorption of Small Organic Molecules on Graphene. *J. Amer. Chem. Soc.* **2013**, *135*, 6372-6377. DOI: 10.1021/ja403162r.

14 Perdew, J. P.; Schmidt, K. Jacob's Ladder of Density Functional Approximations for the Exchange-Correlation Energy, *AIP Conf. Proc.* **2001**, *577*, 1-20. DOI: 10.1063/1.1390175.

15 Takeuchi, K.; Yamamoto, S.; Hamamoto, Y.; Shiozawa, Y.; Tashima, K.; Fukidome, H.; Koitaya, T.; Mukai, K.; Yoshimoto, S.; Suemitsu, M.; Morikawa, Y.; Yoshinobu, J.; Matsuda,

I. Adsorption of CO_2 on Graphene: a Combined TPD, XPS, and vdW-DF Study. *J. Phys. Chem. C* **2017**, *121*, 2807-2814. DOI: 10.1021/acs.jpcc.6b11373

16 Smith, R. S.; Kay, B. D. Desorption Kinetics of Carbon Dioxide From a Graphene-Covered Pt(111) Surface. *J. Phys. Chem. A* **2019**, *123*, 3248-3254. DOI: 10.1021/acs.jpca.9b00674.

17 Perdew, J. P.; Burke, K.; Ernzerhof, M. Generalized Gradient Approximation Made Simple. *Phys. Rev. Lett.* **1996**, *77*, 3865. DOI: 10.1103/PhysRevLett.77.3865.

18 Perdew, J. P.; Burke, K.; Ernzerhof, M. Erratum: Generalized Gradient Approximation Made Simple. *Phys. Rev. Lett.* **1997**, *78*, 1396. DOI: 10.1103/PhysRevLett.78.1396.

19 Becke, A. D. Density-Functional Thermochemistry. III. The Role of Exact Exchange. *J. Chem. Phys.* **1993**, *98*, 5648-5652. DOI: 10.1063/1.464913.

20 Stephens, P. J.; Devlin, F. J.; Chabalowski, C. F.; Frisch, M. J. Ab Initio Calculation of Vibrational Absorption and Circular Dichroism Spectra Using Density Functional Force Fields. *J. Phys. Chem.* **1994**, *98*, 11623-11627. DOI: 10.1021/j100096a001.

21 Lin, Y.-S.; Li, G.-D.; Mao, S.-P.; Chai, J.-D. Long-Range Corrected Hybrid Density Functionals with Improved Dispersion Corrections. *J. Chem. Theory Comput.* **2013**, *9*, 263-272. DOI: 10.1021/ct300715s.

22 Mardirossian, N.; M. Head-Gordon, M. ωB97X-V: A 10-Parameter, Range-Separated Hybrid, Generalized Gradient Approximation Density Functional with Nonlocal Correlation, Designed by a Survival-of-the-Fittest Strategy. *Phys. Chem. Chem. Phys.* **2014**, *16*, 9904-9924. DOI: 10.1039/C3CP54374A.

23 Kozuch, S.; Gruzman, D.; Martin, J. M. L. DSD-BLYP: A General Purpose Double Hybrid Density Functional Including Spin Component Scaling and Dispersion Correction. *J. Phys. Chem. C* **2010**, *114*, 20801-20808. DOI: 10.1021/jp1070852.

24 Goerigk, L.; Hansen, A.; Bauer, C.; Ehrlich, S.; Najibi, A.; Grimme, S. A Look at the Density Functional Theory Zoo with the Advanced GMTKN55 Database for General Main Group Thermochemistry, Kinetics and Noncovalent Interactions. *Phys. Chem. Chem. Phys.* **2017**, *19*, 32184-32215. DOI: 10.1039/C7CP04913G.

25 Neese, F. Software Update: the ORCA Program System, Version 4.0. *WIREs Comput. Mol. Sci.* **2017**, *8*, e1327. DOI: 10.1002/wcms.1327.

26 Matthews, D. A.; Stanton, J. F. Non-Orthogonal Spin-Adaptation of Coupled Cluster Methods: A New Implementation of Methods Including Quadruple Excitations. *J. Chem. Phys.* **2015**, *142*, 064108. DOI: 10.1063/1.4907278.

27 Matthews, D. A.; Cheng, L.; Harding, M. E.; Lipparini, F.; Stopkowicz, S.; Jagau, T.-C.; Szalay, P. G.; Gauss, J.; Stanton, J. F. Coupled-Cluster Techniques for Computational Chemistry: The CFOUR Program Package. *J. Chem. Phys.* **2020**, *152*, 214108. DOI: 10.1063/5.0004837.

28 Larsen, A. S.; Mortensen, J. J.; Blomqvist, J.; Castelli, I. E.; Christensen, R.; Dułak, M.; Friis, J.; Groves, M. N.; Hammer, B.; Hargus, C.; Hermes, E. D.; Jennings, P. C.; Jensen, P. B.; Kermode, J.; Kitchin, J. R.; Kolsbjerg, E. L.; Kubal, J.; Kaasbjerg, K.; Lysgaard, S.; Maronsson, J. B.; Maxson, T.; Olsen, T.; Pastewka, L.; Peterson, A.; Rostgaard, C.; Schiøtz, J.; Schütt, O.; Strange, M.; Thygesen, K. S.; Vegge, T.; Vilhelmsen, L.; Walter, M.; Zeng, Z.; Jacobsen, K. W. The Atomic Simulation Environment—a Python Library for Working with Atoms. *J. Phys.: Condens. Matter* **2017**, *29*, 273002. DOI: 10.1088/1361-648X/aa680e.

29 Parker, T. M.; Burns, L. A.; Parrish, R. M.; Ryno, A. G.; Sherrill, C. D. Levels of Symmetry Adapted Perturbation Theory (SAPT). I. Efficiency and Performance for Interaction Energies. *J. Chem. Phys.* **2014**, *140*, 094106. DOI: 10.1063/1.4867135.

30 Szalewicz, K. Symmetry-Adapted Perturbation Theory of Intermolecular Forces. *WIREs Comput. Mol. Sci.* **2012**, *2*, 254-272. DOI: 10.1002/wcms.86.

31 Hohenstein, E. G.; Sherrill, C. D. Wavefunction Methods for Noncovalent Interactions. *WIREs Comput. Mol. Sci.* **2012**, *2*, 304-326. DOI: 10.1002/wcms.84.

32 Parrish, R. M.; Burns, L. A.; Smith, D. G. A.; Simmonett, A. C.; DePrince, A. E.; Hohenstein, E. G.; Bozkaya, U.; Sokolov, A. Y.; Remigio, R. D.; Richard, R. M.; Gonthier, J. F.; James, A. M.; McAlexander, H. R.; Kumar, A.; Saitow, M.; Wang, X.; Pritchard, B. P.; Verma, P.; Schaefer, H. F.; Patkowski, K.; King, R. A.; Valeev, E. F.; Evangelista, F. A.; Turney, J. M.; Crawford, T. D.; Sherrill, C. D. Psi4 1.1: An Open-Source Electronic Structure Program Emphasizing Automation, Advanced Libraries, and Interoperability. *J. Chem. Theory Comput.* **2017**, *13*, 3185-3197. DOI: 10.1021/acs.jctc.7b00174

33 Smith, D. G. A.; Burns, L. A.; Simmonett, A. C.; Parrish, R. M.; Schieber, M. C.; Galvelis, R.; Kraus, P.; Kruse, H.; Remigio, R. D.; Alenaizan, A; James, A. M.; Lehtola, S.; Misiewicz, J. P.; Scheurer, M.; Shaw, R. A.; Schriber, J. B.; Xie, Y.; Glick, Z. L.; Sirianni, D. A.; O'Brien, J. S.; Waldrop, J. M.; Kumar, A.; Hohenstein, E. G.; Pritchard, B. P.; Brooks, B. R.; Schaefer, H. F.; Sokolov, K.; Patkowski, K.; DePrince, A. E.; Bozkaya, U.; King, R. A.; Evangelista, F. A.; Turney, J. M.; Crawford, T. D.; Sherrill, C. D. Psi4 1.4: Open-Source Software for High-Throughput Quantum Chemistry. *J. Chem. Phys.* **2020**, *152*, 184108. DOI: 10.1063/5.0006002.

34 Weigend, F.; Ahlrichs, R. Balanced Basis Sets of Split Valence, Triple Zeta Valence and Quadruple Zeta Valence Quality for H to Rn: Design and Assessment of Accuracy. *Phys. Chem. Chem. Phys.* **2005**, *7*, 3297-3305. DOI: 10.1039/B508541A.

35 Weigend, F. Accurate Coulomb-Fitting Basis Sets for H to Rn. *Phys. Chem. Chem. Phys.* **2006**, *8*, 1057-1065. DOI: 10.1039/B515623H.

36 Giannozzi, P.; Baseggio, O.; Bonfà, P.; Brunato, D.; Car, R.; Carnimeo, I.; Cavazzoni, C.; de Gironcoli, S.; Delugas, P.; Ruffino, F. F.; Ferretti, A.; Marzari, N.; Timrov, I.; Urru, A.; Baroni, S. Quantum ESPRESSO toward the Exascale. *J. Chem. Phys.* **2020**, *152*, 154105. DOI: 10.1063/5.0005082.

37 Corso, A. D. Pseudopotentials Periodic Table: From H to Pu. *Comput. Mater. Sci.* **2014**, *95*, 337-350. DOI: 10.1016/j.commatsci.2014.07.043.

38 Riplinger, C.; Neese, F. An Efficient and Near Linear Scaling Pair Natural Orbital Based Local Coupled Cluster Method. *J. Chem. Phys.* **2013**, *138*, 034106. DOI: 10.1063/1.4773581.

39 Neese, F. Prediction of Molecular Properties and Molecular Spectroscopy with Density Functional Theory: from Fundamental Theory to Exchange-Coupling. *Coord. Chem. Rev.* **2009**, *253*, 526-563. DOI: 10.1016/j.ccr.2008.05.014.

40 Neese, F.; Schwabe, T.; Grimme, S. Analytic Derivatives for Perturbatively Corrected "Double Hybrid" Density Functionals: Theory, Implementation, and Applications. *J. Chem. Phys.* **2007**, *126*, 124115. DOI: 10.1063/1.2712433.

41 Nishimura, Y.; Tsuneda, T.; Sato, T.; Katouda, M.; Irle, S. Quantum Chemical Estimation of Acetone Physisorption on Graphene Using Combined Basis Set and Size Extrapolation Schemes. *J. Phys. Chem. C* **2017**, *121*, 8999-9010. DOI: 10.1021/acs.jpcc.6b13002.

42 Feller, D.; Jordan, K. D. Estimating the Strength of the Water/Single-Layer Graphite Interaction. *J. Phys. Chem. A* **2000**, *104*, 9971-9975. DOI: 10.1021/jp001766o.

43 Grimme, S.; Mück-Lichtenfeld, C.; Antony, J. Noncovalent Interactions between Graphene Sheets and in Multishell (Hyper)Fullerenes. *J. Phys. Chem. C* **2007**, *111*, 11199-11207. DOI: 10.1021/jp0720791.

44 Antony, J.; Grimme, S. Structures and Interaction Energies of Stacked Graphene–Nucleobase Complexes," *Phys. Chem. Chem. Phys.* **2008**, *10*, 2722-2729. DOI: 10.1039/B718788B.

45 Gryn'ova, G.; Corminboeuf, C. Steric "Attraction": not by Dispersion Alone. *Beilstein J. Org. Chem.* **2018**, *14*, 1482-1490. DOI: 10.3762/bjoc.14.125.

TOC Image